RSC Advances

ROYAL SOCIETY OF CHEMISTRY

www.rsc.org/advances

RSC Advances

Dynamic Article Links ►

Cite this: DOI: 10.1039/c0xx00000x

www.rsc.org/xxxxxx

Full Paper

Carbon Nanotubes based Polymer Nanocomposites: Biomimic Preparation and Organic Dye Adsorption Applications

Yili Xie[a,c], Chengbin He[a], Leichun Liu[a], Liucheng Mao[a], Ke Wang[b], Qiang Huang[a], Meiying Liu[a], Qing Wan[a], Fengjie Deng[a], Hongye Huang[a], Xiaoyong Zhang[a,*], Yen Wei[b,*]

Received (in XXX, XXX) Xth XXXXXXXXX 200X, Accepted Xth XXXXXXXXX 200X

DOI: 10.1039/b000000x

The development of high efficient adsorbents for removal of organic dyes from wastewater has attracted much attention recently. Surface modification of adsorbents with polymers is a general strategy for enhancement of their adsorption capability. In this work, a novel strategy that combination of mussel inspired chemistry and SET-LRP has been developed for fabrication of high efficient adsorbents, poly(sodium p-styrene sulfonate) modified the muti-walled carbon nanotubes (CNTs) for the first time. The adsorption applications of these CNTs based polymer nanocomposites for removal of cationic dyes (methylene blue, MB) from water solution were also examined. The successful preparation of these CNTs based polymer nanocomposites was confirmed by a series of characterization techniques. Furthermore, the influence of adsorption parameters including contact time, concentration of MB, adsorption temperature and time has been investigated. According to the experimental data, the adsorption capacity of MB was in direct proportion to the contact time, while in inverse proportional to the temperature. The maximum absorption capacity of MB for CNTs-PDA-PSPSH was even arrived 160 mg g^{-1}, demonstrating excellent adsorptive property of functional CNTs for MB. The method described in this work for the preparation of CNTs based polymer nanocomposites is simple, effective and general, that should be a universal strategy for preparation of high efficient adsorbents for environmental applications.

1. Introduction

Dye industries, including plastics, cosmetics, pulp manufacture, textiles, pharmaceuticals and food processing, have been rapid development in recent years. Dyestuffs are water-soluble organic matters that can be converted into solution and enable to make fiber materials or other substances obtain bright and solid color.[1] Among the production process of colorful dyes, the fact that a part of poisonous organic materials have transferred to the wastewater, resulting in a large amount of aromatic, polycyclic aromatic or heterocyclic compounds exist in the water and be harmful to human health.[2-4] On the one hand, as organic compounds with stable structure, dyestuffs could stay in the environment for a long retention period.[5] On the other hand, various aromatic compounds with complicate structure are existed in dye wastewater, resulting in difficult points of wastewater treatment due to their high colority, concentration, stable nature and not easy to degrade. Therefore, more and more attentions have been paid to treat the dye industrial wastewater before discharge in recent years.[6-12]

In theory, a variety of physical, chemical and biological methods can be used for the removal of dye contained wastewater. For instance, coagulation sedimentation, ion exchange, ultrafitration, dialysis, chemical oxidation and electrochemical have ever been applied in dye wastewater treatment.[13] However these methods could make effective and economic benefit only in high concentrations, and there are disadvantages reflected in energy consuming, high cost and may generate large amounts of toxic or carcinogenic byproducts.[13-20] To the best of our knowledge, adsorption has proven to be a hot and attractive method for removal of dye contained wastewater due to the economic effectiveness and low operation cost.[21-28] In the past decades, there are many studies have been reported about removal of heavy metal ions and organic dyes using active carbon, natural fibers, minerals *etc* as adsorption materials.[29] Unfortunately, most of these adsorbents have relative low adsorption capacity. It is therefore surface modification of the adsorbents to improve the adsorption capability of these adsorbents have been intensively pursued recently.[30]

As a star member of carbon family, carbon nanotubes (CNTs) with nano-size diameter and tubular microstructure, have been the worldwide hotspot of research in various fields such as electronic devices, composites hydrogen storage, catalysis and drug delivery since their first discovery in 1991.[31-35] Furthermore, because of excellent structural features and high surface areas, many attentions have been paid to the removal of heavy metal ions (Cu^{2+}, Zn^{2+}, Cd^{2+}, Pd^{2+}, Cr^{6+} and fluoride) and different organic matters existed in environmental wastewater using CNTs as adsorbents.[36-39] More importantly, as compared with the usual adsorbents like activated carbon, research found that CNTs showed higher efficiency for the removal of both heavy mental

ions and dye wastewater because of their unique performance.[40, 41] Although the excellent performance, poor dispersibility in aqueous solution and absence of functional groups of CNTs have been pivotal limitation and followly resulted in low adsorption performance. Therefore, the development of facile methods for modifying CNTs to improve their water dispersibility and adsorption performance is extremely desirable.[42-45]

As a facile and versatile surface modification method, mussel inspired chemistry has received increasing attentions because of its simpilicity and availability for the surface modification of materials regardless of their size, shape and compositions. Mussel inspired surface modification was inspired from the marine mussels, whose excretions are mussel adhesive proteins (MAPs). These unique proteins make mussels possess strong adhesion force toward various materials.[46-52] To be clear, the major component of MAPs is 3,4-Dihydroxyphenyl-L-alanine (DOPA) which participates in the intermolecular cross-linking reaction.[53-56] Therefore, mussel inspired surface modification strategy was reported by Lee *et al* in 2007, they demonstrated that dopamine possess similar function of MAPs, which could be self-polymerized under alkaline condition and formed polydopamine (PDA) coating on the material surface.[49, 57-61] More importantly, the special functional groups such as amino and hydroxyl could be introduced onto the surface of materials, providing foundation for the introduction of functional components to the materials.[62] For example, our group has reported that a novel strategy for the surface modification of CNTs via combination of mussel inspired chemistry and Single-Electron Transfer Living Radical Polymerization (SET-LRP) to improve the dispersibility of CNTs in aqueous solution.[63]

In this study, PDA and sodium p-styrenesulfonate hydrate (SPSH) were selected to modify pristine CNTs via an original strategy combine with the mussel-inspired chemistry and SET-LRP. The concrete process was clearly shown in **Scheme 1**. First, the CNTs-PDA could be prepared by the self-polymerized of dopamine to form the PDA coating on the surface of CNTs under alkaline solution based on mussel-inspired chemistry. Secondly, the SET-LRP initiator (CNTs-PD-Br) was synthesized via amidation and esterification using CNTs-PDA and 2-bromo-2-methylpropionyl bromide as reactants. Finally, polymeric chains were grew on the CNTs-PDA surface to prepare CNTs-PDA-PSPSH using Sodium p-styrenesulfonate hydrate as monomer. Thus obtained functional CNTs show great water dispersibility. On the other hand, the functionalized CNTs-PDA-PSPSH was used as the adsorbents to remove methylene blue (MB). Various adsorption parameters such as contact time, temperature, pH and initial MB concentration.

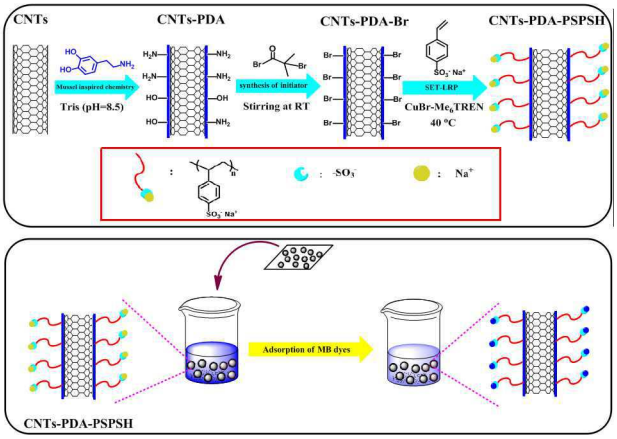

Scheme 1 Schematic representation for the preparation of CNTs-PDA-PSPSH via the combination of mussel-inspired chemistry and facile SET-LRP polymerization method.

2. Experiment

2.1 Materials

Multi-walled carbon nanotubes (CNTs), manufactured by the nanopowder Co. The dopamine hydrochloride was purchased from Sangon Co. Tris-(chydroxymethyl)-aminethane (Tris) (>99%) was obtained from Tianjin Heowns. SPSH (MW:206.19 Da, 90%) was obtained from Aladdin (Shanghai, China) without further purification. Deionized water was prepared for the usage of solution. MB was also purchased from Aladdin.

2.2 Characterization

The synthetic materials were characterized by Fourier transform infrared spectroscopy (FT-IR) using KBr pellets, The FT-IR spectra were supplied from Nicolet5700 (Thermo Nicolet corporation). Transmission electron microscopy (TEM) images were obtained from a Hitachi 7650B microscope operated at 80 kV, the TEM specimens were got by putting a drop of the nanoparticle ethanol suspension on a carbon-coated copper grid. Thermal gravimetric analysis (TGA) was conducted on a TA instrument Q50 with a heating rate of 10 °C min^{-1} under N_2 atmosphere using Aluminum crucibles. Samples weighing between 10 and 20 mg were heated from 25 to 600 °C in N_2 flow (60 mL min^{-1}). N_2 as the balance gas (40 mL min^{-1}). Each sample was ultrasonicated for 30 min prior to analysis. The X-ray photoelectron spectra (XPS) were performed on a VGESCALAB 220-IXL spectrometer using an Al Kα X-ray source (1486.6 eV). The energy scale was internally calibrated by referencing to the binding energy (Eb) of the C1s peak of a carbon contaminant at 284.6 eV.

2.3 Synthesis of CNTs-PDA

CNTs-PDA was prepared according to our previous method.[37] The pure CNTs (1) was added to the Tris buffer solution (30 mL, 10 mM, pH = 8.5) and ultrasonic treatment for 10 min. In the next moment, the dopamine (1.5) was dissolve in 10 mL of Tris buffer solution and put into above-mentioned CNTs Tris solution and stirring at room temperature for 4 h. The CNTs coated with PDA and Tris buffer solution were separated by centrifugation at 8000 rpm for 10 min (Shuke Centrifuge TG-16, Sichuan shuke instrument Co., ltd., China). Precipitation was washed with

distilled water and ethanol three times and dried at 40 °C for 12 h.

2.4 CNTs-PDA-Br

The Br-contained initiators were introduced to the surface of CNTs-PDA through amidation and esterification between CNTs-PDA materials and 2-bromo-2-methylpropionyl bromide. Dry CNTs-PDA (300 mg), TEA (60 mg) and toluene (40 mL) were added to the reaction bottle under N_2, and followly put into ice-water bath. When the temperature achieve to 0-5 °C in flask, the solution of 2-bromo-2-methylpropionyl bromide (30 mg) was added into flask. The reactive system was stirred for 4 h at 0 °C. Resulting materials was separated from toluene solution by centrifugation at 8000 rpm for 10 min. The obtained Br-containing initiating groups of materials was vigorously washed with acetone three times to remove residual reactants and dried at 50 °C for further experiment.

2.5 Preparation of CNTs-PDA-PSPSH

The synthesis of high-efficiency adsorbents based on functional CNTs-PDA with hydrophilic polymers via combination of mussel inspired chemistry and SET-LRP using SPSH as the monomer was clearly described in follows: 1 g CNTs-PDA-Br, 2 g SPSH monomer, 80 mg CuBr were added into the polymerization bottle mixed with 10 mL DMF and 10 mL acetonitrile. The mixture was under ultrasonic treatment for 10 min and then stirred in oil both for 10 min at 40 °C. The catalytic Me6TREN in DMF (2 mL) was injected into the polymerization bottle using gas syringe. After 8 h stirring, the reactive products were centrifuged to wipe off the organic solution and washed with water for three times, and then dried at 50 °C for 48 h. The solution of EDTA (5 mol/L) was used for the removal of the residual Cu^{2+} in the CNTs-PDA-PSPSH. Ultimately, the absolute CNTs-PDA-PSPSH was obtained for further characterization and a series of adsorption experiments.

2.6 Adsorption experiment

Batch adsorption experiments were carried out using 50 mL sample tubes with the addition of 10 mg modified adsorbent CNTs-PDA-PSPSH and MB solution (50 mg/L). Kinetic experiments were completed by the constant initial concentration (50 mg/L) of MB solution at room temperature and pH (7.0). The study of adsorption isotherms carried out by adding the same amount of adsorbent into 40 mL MB solution with different initial concentration from 5 to 500 mg/L at 25 °C and pH (7.0).

The concentrations of MB remained in supernatant solutions after different reactive time were determined using UV-vis spectrophotometer (**Fig. S1 and Fig. S2**). It can be seen that the adsorption values of MB solutions is in direct proportion to the concentrations of MB solutions. And the concentrations of unknow MB solutions can be calculated using the following formula $Ce = 76.21 \times Abs.$ Ce is the concentration of MB solution, and Abs is the adsorption of MB solution. The adsorption capacity (Q_e, mg/g) and the MB removal efficiency (R %) were analyzed by the following equation, respectively:

$$Q_e = \frac{(C_0 - C_t)V}{m}$$

$$R = \frac{100(C_0 - C_t)}{C_0}$$

Where C_0 (mg/L) is the initial concentration of MB solution and C_t is the equilibrium MB concentration. V (mL) is the dye MB solution volume, m (mg) is the adsorbent dose, Q_e (mg/g) is the adsorption capacity at the equilibrium time. And R (%) is the removal efficiency of the MB solution. The effect of temperature studied by 5 °C gradient of temperature from room temperature 25 °C to 55 °C, keeping the other reactive condition remain unchanged. The effect of pH was performed by adding 10 mg adsorbent into 40 mL MB solution in the condition of different pH in the range from 2 to 10. The initial pH values of MB solution were adjusted by using 0.1 mol/L NaOH or 0.1 mol/L HCl solutions.

3. Results and discussion

3.1 Characterization of CNTs-PDA-PSPSH

The new CNT-polymer hybrid materials were prepared for removal of MB via combination of mussel inspired chemistry and SET-LRP method in this work. These CNT-PDA-PSPSH adsorbents show excellent adsorption capability for MB organic dyes which is widely used in the coloring paper, dyeing cottons, wools and coating for paper stock. The surface modification of CNTs by the PDA coating was carried out in alkaline solution due to self-polymerization of dopamine. Afterwards, the hydrophilic polymer (PSPSH) was directly grew on the surface of CNTs-PDA by SET-LRP. The successful modification of CNTs could be confirmed by a series of characterization measurements such as TEM, FT-IR, TGA and XPS. The morphology of pristine CNTs and functional CNTs with PDA and polymer could be clearly noticed from TEM images. The diameter of pristine CNTs was approximately 30-40 nm, which was characterized by our previous report.[37] After surface modification of CNTs with dopamine in alkaline solution, the PDA films attached on the CNTs with thickness about 10 nm can be observed, demonstrating that successful surface modification of CNTs via mussel inspired chemistry (**Fig. S3**). After further functionalization with hydrophilic polymers by SET-LRP method, the thickness of polymer films on the CNTs was further increased, that was calculated to be approximately 30 nm. These results implied that PSPSH was successfully grew on the surface of CNTs.

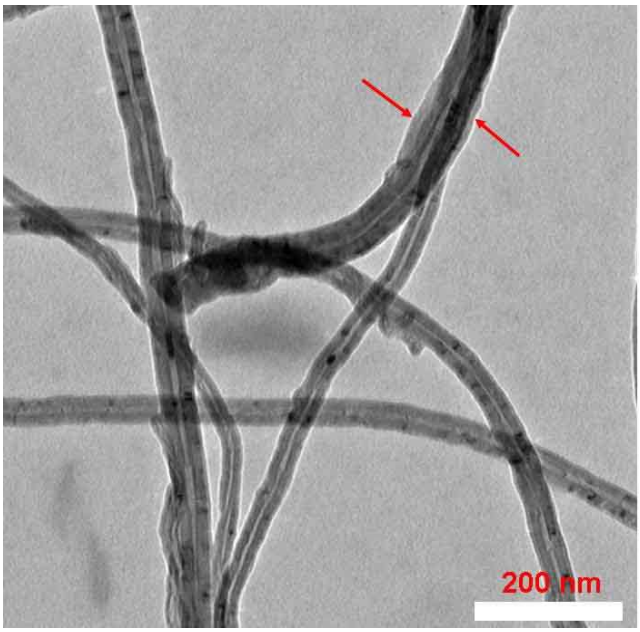

Fig.1 Representative TEM images of CNTs-PDA-PSPSH. Scale bar = 200 nm. The successful modification of CNTs surface with PDA and polymer coating could be clearly observed, demonstrating that successful preparation of adsorbents (CNTs-PDA-PSPSH) via combination of mussel inspired chemistry and SET-LRP method.

As mentioned above, FT-IR, TGA, XPS characterization techniques were as well employed to further verify the successful preparation of CNTs-PDA-PSPSH. With the purpose of determining the chemical groups of the adsorbent CNTs-PDA-PSPSH, the measurement of FT-IR spectra was carried out. As shown in **Fig. 2**, the FT-IR spectra of pristine CNTs shows that there is few specific functional groups. After the first synthesis step that coating PDA films on the surface of CNTs on the basis of mussel-inspired chemistry, the fact that successful modification of CNTs-PDA can be proved by the legible peak at 3445 cm^{-1}, which was ascribed to the stretching vibration of -NH_2. And the stretching vibration of -CH_2 existed in PDA films located at 2859 cm^{-1}, which could be observed in **Fig. 2** (red line), further indicated that successful synthesis of the CNTs-PDA. Ultimately, as for the FT-IR spectra as regard to the CNTs-PDA-PSPSH, the most representative evidence for the resoundingly modification of CNTs-PDA surface with polymer was that the appearance of new peak at 1184 cm^{-1} (S=O) and the disappearance of –NH_2 at 3445 cm^{-1}. Furthermore, a series of obvious peaks ranged from 500 to 1000 cm^{-1} were primarily appeared, which represented the introduction of abundant benzene rings, providing powerful evidence that successful growth of PSPSH polymer by SET-LRP method. Therefore, we concluded that successful preparation of CNTs-PDA-PSPSH via combination of mussel inspired chemistry and SET-LRP strategy.

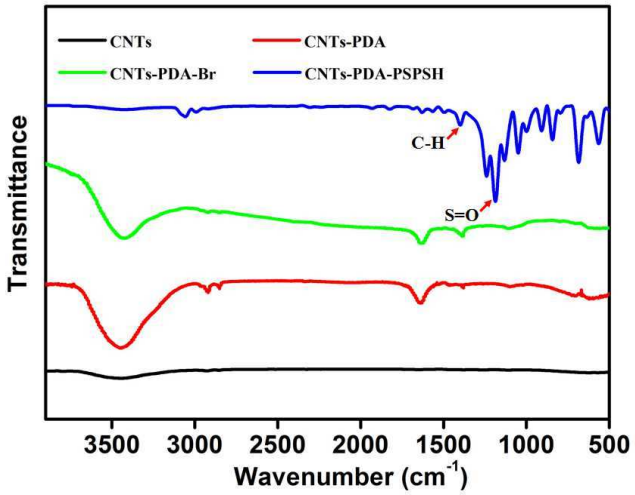

Fig. 2 FT-IR spectra of CNTs, CNTs-PDA, CNTs-PDA-Br and CNTs-PDA-PSPSH

TGA was used to analyze the content of each polymer on CNTs-PDA-PSPSH. From the **Fig. 3**, the weight loss of unmodified CNTs was about 2.75% when temperature was heated from 100 to 600 °C, which indicated the splendid thermal stability of pristine CNTs. Comparing with the pristine CNTs, the obvious weight loss of CNTs-PDA and CNTs-PDA-Br samples can be observed. When the temperature was raised from 100 up to 600 °C, the mass loss of CNTs-PDA was calculated about 13.52%, suggesting that successful cover of PDA on the CNTs via mussel inspired chemistry. And comparing with weight loss of pure CNTs, the weight percentage of PDA film attached onto the CNTs surface could calculate about 10.82%. Especially, the weight loss of CNTs-PDA became much rapidly when temperature was increase from 151 to 446 °C, which can be ascribed to the decomposition of C-O. On the other hand, a small weight loss could be noticed from 450 to 590 °C, which could be attributed to the decomposition of stable benzene rings. As compared with CNTs-PDA, the weight loss percentage was further increased in the smaple of CNTs-PDA-PSPSH. The weight loss of CNTs-PDA-PSPSH was arrived 20.25% when the temperature was up to 600 °C. Therefore, we can further conclude that PSPSH can be facilely introduced on the surface of CNTs through combination of mussel inspired chemistry and SET-LRP.

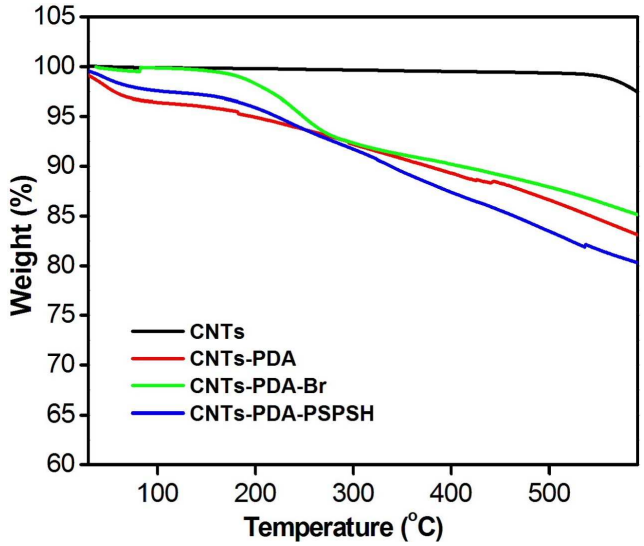

Fig. 3 TGA curves of CNTs, CNTs-PDA, CNTs-PDA-Br and CNTs-PDA-PSPSH under N_2 atmosphere

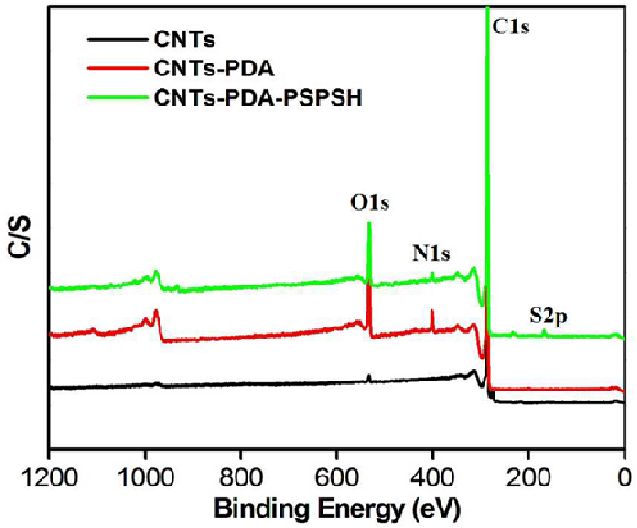

Fig. 4 The XPS curves of CNTs, CNTs-PDA and CNTs-PDA-PSPSH. Survey scans ranged from 0 to 1200 eV.

The XPS curves of CNTs sample is used for the further determination of successful surface modification of CNTs with PDA and PSPSH. The different elements existed in a series of CNT samples could be detected by the survey scanning of XPS spectra between 0 to 1200 eV. Elements existed in CNT samples contained Carbon (C), Nitrogen (N), Oxygen (O) and Sulfur (S). As shown in the **Fig. 4**, the main peaks at 196.8, 284.0, 533.5 and 400.0 eV, which represent the signal of S2p, C1s, O1s, N1s, respectively. New signals (N1s and O1s) were initially appeared in the samples of CNTs-PDA, while there were no nitrogen and oxygen signals in pristine CNTs, suggesting that successful modification of CNTs with PDA films via mussel-inspired chemistry. After conjugating the PSPSH onto the surface of CNTs-PDA by typical SET-LRP method, the new signal appeared at 196.87 eV was attributed to the S2p, demonstrating that PSPSH polymers were directly grew onto the surface of CNTs-PDA. Furthermore, the singals represented C1s and O1s for the CNTs-PDA-PSPSH were enhanced, which could be explained that the introduction of polymers contained numerous carbon and oxygen elements. These results suggested that SET-LRP is a reliable method for the import of PSPSH polymers to the CNT surface. These results provide direct evidence that successful surface modification of CNTs with PDA films and PSPSH polymers via combination of mussel inspired chemistry and SET-LRP polymerization method.

The XPS curves of high resolution S2p, C1s, N1s and O1s were shown in **Fig. 5**. As shown in **Fig. 5A**, the new element appeared at 196.87 eV, which represented the S existed in the PSPSH, demonstrating that successful conjugation of PSPSH on the modified CNTs surface with PDA. As shown in **Fig. 5B**, three peaks with similar morphology but different intensity were located at 284.83 eV, which could be contributed to the sp3-hybridised of carbon atom. Furthermore, the C1s signal of CNTs-PDA-PSPSH was obviously enhanced comparing with CNTs and CNTs-PDA. The possible reason is introduction of polymers contained numerous carbon atoms. According to the **Fig. 5C**, the peak located at 400.35 eV could serve as the N1s signal. A strong peak was appeared in the sample of CNTs-PDA, which was never appeared in the pristine CNTs, suggesting that PDA coating successfully coated on the CNTs surface via mussel inspired chemistry. Furthermore, We can noticed that signal intensity of CNTs-PDA-PSPSH is weaker than CNTs-PDA, this phenomenon could be explained that the formation of polymer films on the CNTs-PDA surface, which leads to be difficult penetrated by X-ray. **Fig. 5D** shows the O1s XPS curves of CNT samples. It can be seen that intensity of O1s XPS signal was significantly enhanced in the samples of CNTs-PDA and CNTs-PDA-PSPSH, further confirming that successful surface modification of CNTs with PDA and PSPSH based on the combination of mussel inspired chemistry and SET-LRP.

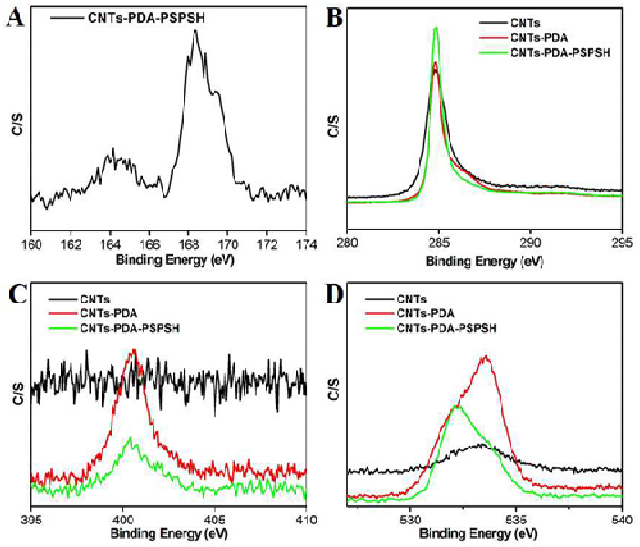

Fig. 5 The representative XPS curves of CNTs, CNTs-PDA and CNTs-PDA-PSPSH. (A) S2p region, (B) C1s region, (C) N1s region and (D) O1s region

3.2 Adsorption experiment studies

3.2.1 Effect of contact time and adsorption kinetics

Fig. 6 shows the experimental result of contact time on the adsorption capacity of MB onto the pristine CNTs and the prepared CNTs-PDA-PSPSH at room temperature and the same initial dye concentration of 50 mg/L.[64] As compared with the two curves in **Fig. 6**, it can be easily observed that the equilibrium adsorption quantity of MB on pristine CNTs is approximately 120 mg/g. However, the adsorption process on CNTs-PDA-PSPSH reached up to the equilibrium with less time and more adsorption quantity, which is promote to 174 mg/g under the same adsorption conditions. As MB is an ideally planar molecule with plenty of aromatic rings and CNTs-PDA-PSPSH contain abundant aromatic nucleus as well, the π-π stacking interactions could occur between MB molecules and CNTs-PDA-PSPSH. Furthermore, the electrostatic attraction between MB molecules and CNTs-PDA-PSPSH also plays a key role due to the cationic dyes and the sulfonate ions. Adsorption kinetic studies are completely explored at the same conditions of room temperature and neutral pH value. **Fig. 7** show three kinetic models for the adsorption process, including Pseudo-first-order, Pseudo-second-order and Intro-particle diffusion model. These non-liner form of the kinetic models can be expressed as follows:

$$Q_t = Q_e(1 - e^{-k_1 t})$$

$$Q_t = \frac{k_2 Q_e^2 t}{1 + k_2 Q_e t}$$

$$h = k_2 Q_e^2$$

Where Qt (mg/g) is the quantity of MB adsorbed by CNTs-PDA-PSPSH at different contact time t (min), Qe (mg/g) is the equilibrium adsorption capacity, K_1 (min^{-1}) and K_2 ($g \cdot mg^{-1} \cdot min^{-1}$) are the equation rate constant for Pseudo-first-order and Pseudo-second-order, respectively. h (mg/g min) is the initial adsorption rate of the MB adsorption process on Pseudo-second-order model. And the value of these parameters and the correlation coefficient (R^2) are listed in **Table 1**.

In this study, the Intro-particle diffusion model also involved in the adsorption process. The equation is expressed as the equation below:

$$Q_t = k_p t^{0.5}$$

Where Qt (mg/g) is the quantity of MB, and Kp ($mg \cdot g^{-1} \cdot min^{-0.5}$) is the equation rate constant. And the calculation result listed in **Table 1** as well. It can be observed from **Table 1** that the correlated coefficient (R^2) from Pseudo-first-order is 0.995, which is comparatively higher than the other two kinetic models, while the Pseudo-second-order R^2 = 0.975 is also relatively high. On the other hand, the results indicated that the adsorption consequence better fitted the Pseudo-first-order than the Pseudo-second-order, which illustrates that Pseudo-first-order rate equation can be properly ascribed to the kinetic adsorption model. The adsorption involved in different reaction rate steps. Initially rapid and then slow may attribute to the decrease of the adsorbent monolayer sites and the reduction of the MB concentrations.

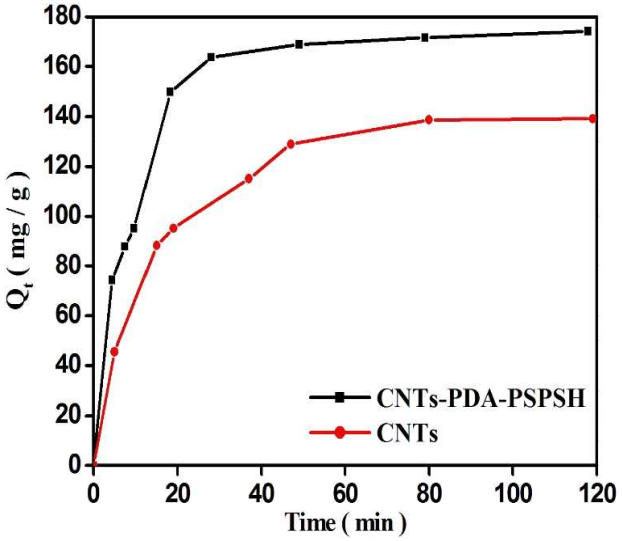

Fig. 6 The effect of contact time on the adsorption of the MB using CNTs and CNTs-PDA-PSPSH as adsorbents. It can be seen that the adsorption capability of CNTs-PDA-PSPSH is obviously higher than that of pristine CNTs.

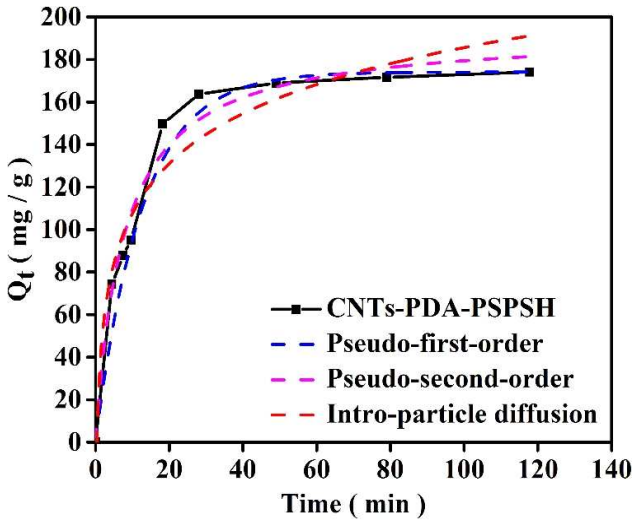

Fig. 7 The adsorption kinetics of CNTs-PDA-PSPSH.

Table 1 Data of Pseudo-first-order, Pseudo-second-order and Intra-particle diffusion

Models	Parameters	Initial concentration(mg/L)
		10
Pseudo-first-order	$Q_{e\,(cal)}$ (mg/g)	174
	K_2 (min^{-1})	0.0933
	R^2	0.995
Pseudo-second-order	$Q_{e\,(cal)}$ (mg/g)	194
	K_2 ($g \cdot mg^{-1} \cdot ming^{-1}$)	0.000677
	h ($mg \cdot g^{-1} \cdot ming^{-1}$)	25.2
	R^2	0.975
Intra-particle diffusion	Kp ($mg \cdot g^{-1} \cdot min^{-1/2}$)	2.7×10^{7}
	R^2	0.825

3.2.2 Effect of temperature and thermodynamic study

Fig. 8A shows the dye adsorbed onto CNTs-PDA-PSPSH at different temperatures. The initial contact time was selected as 120 min and the MB concentration was 50 mg/L. The MB adsorption capacity assume a remarkable increasing tendency with the decrease in the experiment temperature at the range of 298 to 330 K. And at the equilibrium time, the adsorption capacity of MB solution can reach up to 151 mg/g at 298 K. As shown in **Fig. 8B**, the linear relation between the 1/T and ln (Qe/Ce), which also help to verify the experimental results. It can be concluded that the MB adsorption on the modified adsorbent CNTs-PDA-PSPSH is favored at lower temperatures within the temperature range and the CNTs-PDA-PSPSH can perform a better efficiency of the MB solution removal.

Thermodynamics parameters including enthalpy change (△H⊙), Gibbs free energy (△G⊙) and entropy change (△S⊙) were chosen to estimate the effect of temperature on MB adsorption and offer the adsorption mechanism and behavior between the MB solution and modified adsorbent. They can be determined by the following equations:

$$\ln K\alpha = \frac{\Delta S^{o}}{R} - \frac{\Delta H^{o}}{R \cdot T}$$

$$K\alpha = \frac{Q_e}{C_e}$$

$$\Delta G^{o} = -RT\ln K\alpha$$

Where Kα and R (8.314 J/mol•K) are the constant of the equations; T is the MB solution temperature (K). The plot of lnKα as the function of 1/T, △H⊙ and △S⊙ were calculated from the slope and intercept from the Van't Hoff plots of lnKα with 1/T, respectively. The calculated thermodynamic parameters were listed in **Table 2**. The negative value of △H⊙ confirms the adsorption process is an exothermic reaction, which is correspond to the effect of temperature. In addition, the value of △G⊙ indicates the spontaneous process and the feasibility of the adsorption on MB solution by the original modified CNTs-PDA-PSPSH. More importantly, the increase of negative value of △G⊙ with the increasing temperature illustrate the adsorption is more favorable at lower temperature, which is consistent with the above described conclusion.

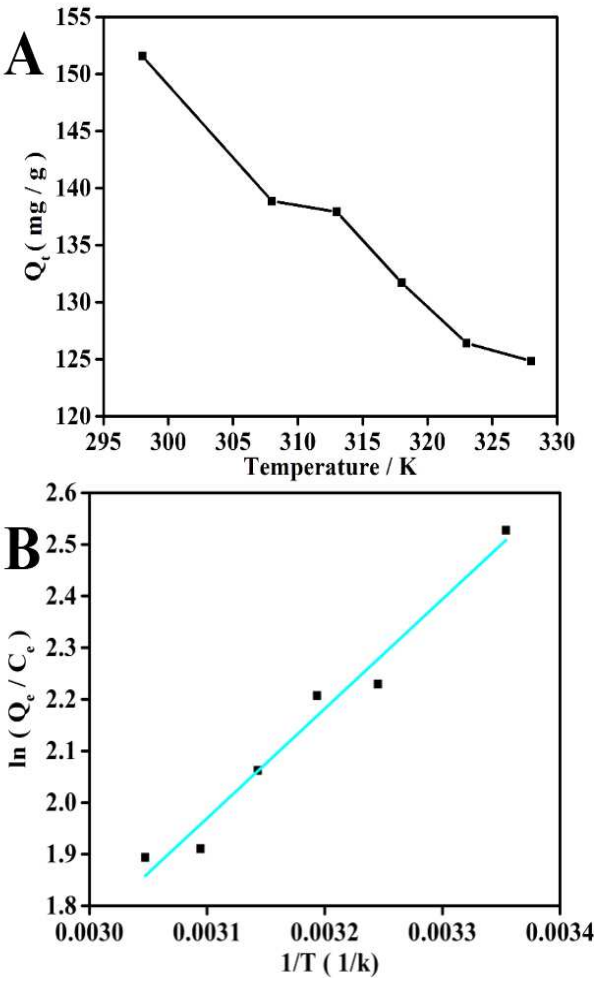

Fig. 8 (A) The effect of temperature on the adsorption of MB organic dyes by CNTs-PDA-PSPSH. Experimental condition: CMB = 50 mg/L, pH = 7.0, t = 120 min. (B) Van't Hoff plot for the adsorption of the MB by CNTs-PDA-PSPSH

Table 2 Data of the thermodynamic parameters for the adsorption of MB by CNTs-PDA-PSPSH

T (K)	ΔG^0 (KJ/mol·K)	ΔH^0 (KJ/mol·K)	ΔS^0 (KJ/mol·K)
298	-6.26	-17.6	-0.0383
308	-5.71	-17.5	
313	-5.74	-17.7	
318	-5.45	-17.6	
323	-5.13	-17.5	
328	-5.17	-17.7	

3.2.3 Effect of pH

The effect of initial solution pH on MB removal by CNTs-PDA-PSPSH was studied within a certain range between 2 to 11, which is because dopamine would alter the properties under higher pH conditions. As shown in **Fig. 9**, the adsorption capacity of MB solution just have a few small fluctuations, the lowest capacity is 153 mg/g and the highest was up to 179 mg/g. As far as that was concerned, the adsorption tendency presented a relatively stable superior scope, which indicated that the influence factor of pH on the reaction did not exert a tremendous influence. Compared with the other similar adsorption literature consequences, the following results of this study can be in touch with the two reasons, the one is new choice of an original high polymer containing the sulfonate ions modified on the pristine CNTs and the other is adsorption mechanism of the MB solution on CNTs-PDA-PSPSH. In another aspect, the results that the adsorption capacity remain at the same level maybe a better phenomenon because the capacity of the adsorbents keep at almost the highest within the topmost removal efficiency corresponding to the same consequence above of the impact factor of contact time. It signified that the pH parameter could not influence or debase the adsorption performance of the CNTs-PDA-PSPSH, which indicated that the modified adsorbent CNTs-PDA-PSPSH could be appropriate for the MB solution of a wide pH range.

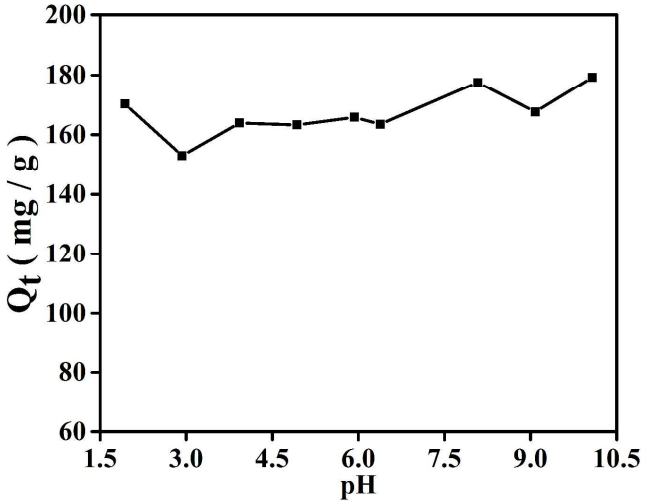

Fig. 9 The influence of solution pH values for the adsorption capacity of CNTs-PDA-PSPSH for MB.

3.2.4 Adsorption isotherms

On the basis of a series of adsorption experimental data, the adsorption capacity on modified CNTs-PDA-PSPSH was considerable. Herein adsorption isotherm were bring into explore the adsorption process and mechanisms. Langmuir isotherm and Freundlich isotherm models, which are two common models utilized in adsorption field, were both introduced in this study to investigate the surface properties and affinity of the dye MB removal on CNTs-PDA-PSPSH. The Langmuir isotherm model based on the description that the adsorption process between MB and adsorbent CNTs-PDA-PSPSH occurred on the adsorbent surface active site without any interaction as regard to the adsorbate molecules. The following equation can be best describe Langmuir isotherm model:

$$Q_e = \frac{bQ_m C_e}{1 + bC_e}$$

Where Q_e (mg/g) and Q_m (mg/g) is represented the adsorption capacity at the maximum amount and the equilibrium quantity of the reaction time, respectively. C_e (mg/L) is the equilibrium MB concentration, b (L/mg) is the constant of the adsorption process. The Freundlich isotherm model, which is an empirical isothermal equation in the light of batch experimental data, correspond to the assumption that the mechanism of dye adsorption is heterogeneous systems. And the concrete equation is described as

follows:

$$Q_e = K_F C_e^{\frac{1}{n}}$$

Where Qe (mg/g) is likewise the equilibrium adsorption quantity, Ce (mg/L) is the MB concentration at the equilibrium time of the adsorption, KF [(mg/g) (L/mg) 1/n] is the correlation index of the adsorption process of cationic dye MB on CNTs-PDA-PSPSH, n is the model reactive constant as well.

As the data listed in **Table 3**, the correlation coefficient (R^2) of Langmuir isotherm model is 0.995, which is higher than Freundlich isotherm model (R^2 = 0.984). While both the two correlation coefficient (R^2) are relatively high, but R^2 from Langmuir isotherm model that surpass 0.99 indicated the MB adsorption process was better fitted the Langmuir isotherm model. In this case, the Langmuir model implication and the calculated adsorption capacity from Langmuir model is approaches to the experimental data both can verify the adsorption of MB solution on CNTs-PDA-PSPSH is a monolayer adsorption process. According to Langmuir isotherm, the maxium amount of the removal of MB q_m is 174 mg • g^{-1} for CNTs-PDA-PSPSH. Table 4 listed a comparasion with other reported adsorbents of the q_m value. The result showed the modified material CNTs-PDA-PSPSH is a good adsorbent for the cationic dye removal.

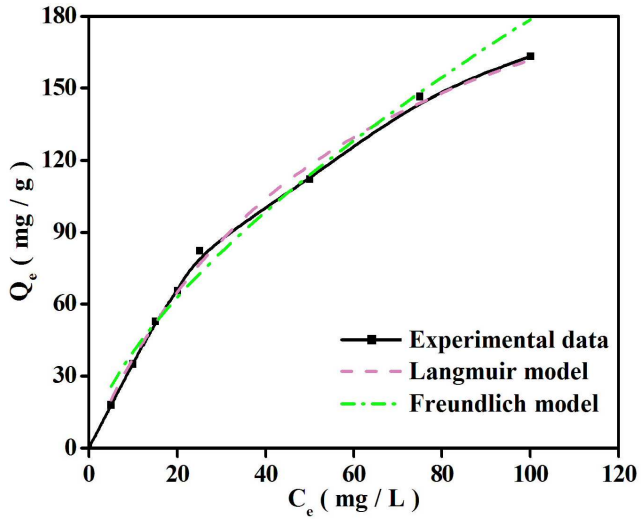

Fig. 10 Adsorption isotherms of MB by CNTs-PDA-PSPSH at initial MB concentration from 20 to 100 mg/L, adsorbent dose 10 mg, pH = 7.0 under room temperature for 120 min.

Table 3 Data of adsorption isotherms of Langmuir and Freundlich model for the adsorption on CNTs-PDA-PSPSH at 298 K

Isotherms	Parameters	Temperatures (K)
		298
Langmuir	Q_0 (mg/g)	7256
	b (L/mg)	0.017
	R^2	0.995
Freundlich	K_F [(mg/g)(L/mg)$^{1/n}$]	9.00
	n	1.54
	R^2	0.984

Table 4 Comparison of adsorption capacity q_m (mg•g^{-1}) of MB on various materials.

Materials	Maximum adsorption capacity qm (mg • g-1)	References
Calcium alginate immobilized graphene oxide	181.81	30
Chitosan/bentonite	95.24	40
Mt	64.43	65
Fe_3O_4/Mt	106.38	65
PDA microspheres	90.7	41
MWCNTs	48.1	44
CNTs-PDA-PSPSH	174	This work

4. Conclusion

In summary, the novel adsorbents with excellent adsorption capacity for MB organic dyes was first prepared via combination of mussel inspired chemistry and SET-LRP. A series of characterization techniques were used to prove the successful preparation of adsorbents (CNTs-PDA-PSPSH). TEM images of CNTs-PDA and CNTs-PDA-PSPSH suggested that the formation of PDA and polymer films on the surface of CNTs. Furthermore, the XPS results of CNT smaples demonstrated that successful modification of CNTs surface with PDA and PSPSH due to the content change of various elements such as S, C, N and O. These analytic results demonstrated this novel strategy described in this work is facile and high-efficient. On the other hand, these synthetic CNTs-PDA-PSPSH was used to adsorb MB organic dyes. A series of influence impacts such as concentrations of MB, temperature, contact time and pH of solution. From the results of adsorption experiments, the adsorption capacity of CNTs-PDA-PSPSH for MB arrived to 174 mg/g within 25 min, suggesting excellent adsorption capacity of CNTs-PDA-PSPSH.

Acknowledgements

This research was supported by the National Science Foundation of China (Nos. 21134004, 21201108, 51363016, 21474057, 21564006, 21561022), and the National 973 Project (Nos. 2011CB935700).

Notes

[a] Department of Chemistry and Jiangxi Provincial Key Laboratory of New Energy Chemistry, Nanchang University, 999 Xuefu Avenue, Nanchang

330031, China. [b] Department of Chemistry and the Tsinghua Center for Frontier Polymer Research, Tsinghua University, Beijing, 100084, P. R. China. [c] Department of Environmental and Chemical Engineering, Nanchang University, 999 Xuefu Avenue, Nanchang 330031, China.
xiaoyongzhang1980@gmail.com; weiyen@tsinghua.edu.cn;
† Electronic Supplementary Information (ESI) available: [TEM images and TGA analysis of CNT samples were provided in supplementary information]. See DOI: 10.1039/b000000x/

References

1. D. Zhao, G. Sheng, C. Chen and X. Wang, *Applied Catalysis B: Environmental*, 2012, **111**, 303-308.
2. E. Errais, J. Duplay, F. Darragi, I. M'Rabet, A. Aubert, F. Huber and G. Morvan, *Desalination*, 2011, **275**, 74-81.
3. Z. Geng, Y. Lin, X. Yu, Q. Shen, L. Ma, Z. Li, N. Pan and X. Wang, *J. Mater. Chem.*, 2012, **22**, 3527-3535.
4. H. A. Harms, N. Tétreault, V. Gusak, B. Kasemo and M. Grätzel, *Phys. Chem. Chem. Phys.*, 2012, **14**, 9037-9040.
5. X. Ren, C. Chen, M. Nagatsu and X. Wang, *Chem. Eng. J.*, 2011, **170**, 395-410.
6. M. Kousha, E. Daneshvar, M. S. Sohrabi, M. Jokar and A. Bhatnagar, *Chem. Eng. J.*, 2012, **192**, 67-76.
7. D. K. Mahmoud, M. A. M. Salleh, W. A. W. A. Karim, A. Idris and Z. Z. Abidin, *Chem. Eng. J.*, 2012, **181**, 449-457.
8. M. A. M. Salleh, D. K. Mahmoud, W. A. W. A. Karim and A. Idris, *Desalination*, 2011, **280**, 1-13.
9. P. Sathishkumar, M. Arulkumar and T. Palvannan, *J. Clean.Prod.*, 2012, **22**, 67-75.
10. H. Zhu, R. Jiang, Y. Q. Fu, J. H. Jiang, L. Xiao and G. M. Zeng, *Appl. Surf. Sci.*, 2011, **258**, 1337-1344.
11. S. Zhang, M. Zeng, J. Li, J. Li, J. Xu and X. Wang, *J. mater. Chem. A*, 2014, **2**, 4391-4397.
12. T. Mondal, A. K. Bhowmick and R. Krishnamoorti, *J. Mater. Chem. A*, 2014, **1**, 8144-8153.
13. K. Yang, W. Wei, L. Qi, W. Wu, Q. Jing and D. Lin, *RSC Adv.*, 2014, **4**, 46122-46125.
14. M. M. Ayad, A. A. El-Nasr and J. Stejskal, *J. Ind. Eng. Chem.*, 2012, **18**, 1964-1969.
15. A. L. Cazetta, A. M. Vargas, E. M. Nogami, M. H. Kunita, M. R. Guilherme, A. C. Martins, T. L. Silva, J. C. Moraes and V. C. Almeida, *Chem. Eng. J.*, 2011, **174**, 117-125.
16. S. K. Das, I. Shome and A. K. Guha, *RSC Adv.*, 2012, **2**, 3000-3007.
17. S. Zhang, J. Li, T. Wen, J. Xu and X. Wang, *RSC Adv.*, 2013, **3**, 2754-2764.
18. G. Zhao, T. Wen, C. Chen and X. Wang, *RSC Adv.*, 2012, **2**, 9286-9303.
19. Y.-P. Zhu, Y.-L. Liu, T.-Z. Ren and Z.-Y. Yuan, *RSC Adv.*, 2014, **4**, 16018-16021.
20. B. Zou, K. Chen, Y. Wang, C. Niu and S. Zhou, *RSC Adv.*, 2015, **5**, 22973-22979.
21. L. Fan, C. Luo, M. Sun, X. Li, F. Lu and H. Qiu, *Bioresource Technol.*, 2012, **114**, 703-706.
22. C. Chen and X. Wang, *Ind. Eng. Chem. Res.*, 2006, **45**, 9144-9149.
23. Q. Zhao, C. Huang and F. Li, *Chem. Soc. Rev.*, 2011, **40**, 2508-2524.
24. J. Li, S. Zhang, C. Chen, G. Zhao, X. Yang, J. Li and X. Wang, *ACS Appl. mater. Inter.*, 2012, **4**, 4991-5000.
25. Y. Sun, S. Yang, G. Sheng, Z. Guo and X. Wang, *J. Environ. Radioactiv.*, 2012, **105**, 40-47.
26. S. Li, L. Qi, L. Lu and H. Wang, *RSC. Adv.*, 2012, **2**, 3298-3308.
27. H. Sun, L. Cao and L. Lu, *Nano. Res.*, 2011, **4**, 550-562.
28. J. Ding, B. Li, Y. Liu, X. Yan, S. Zeng, X. Zhang, L. Hou, Q. Cai and J. Zhang, *J. Mater. Chem. A*, 2015, **3**, 832-839.
29. M. U. Dural, L. Cavas, S. K. Papageorgiou and F. K. Katsaros, *Chem. Eng. J.*, 2011, **168**, 77-85.
30. Y. Li, Q. Du, T. Liu, J. Sun, Y. Wang, S. Wu, Z. Wang, Y. Xia and L. Xia, *Carbohyd. Polym.*, 2013, **95**, 501-507.
31. Q. Wan, J. Tian, M. Liu, G. Zeng, Z. Li, K. Wang, Q. Zhang, F. Deng, X. Zhang and Y. Wei, *RSC Adv.*, 2015, **5**, 25329-25336.
32. X. Zhang, Y. Zhu, J. Li, Z. Zhu, J. Li, W. Li and Q. Huang, *J. Nanopart. Res.*, 2011, **13**, 6941-6952.
33. X. Zhang, J. Yin, C. Peng, W. Hu, Z. Zhu, W. Li, C. Fan and Q. Huang, *Carbon*, 2011, **49**, 986-995.
34. X. Zhang, W. Hu, J. Li, L. Tao and Y. Wei, *Toxicol. Res.*, 2012, **1**, 62-68.
35. X. Zhang, M. Liu, X. Zhang, F. Deng, C. Zhou, J. Hui, W. Liu and Y. Wei, *Toxicol. Res.*, 2015, **4**, 160-168.
36. X. Zhang, J. Ji, X. Zhang, B. Yang, M. Liu, W. Liu, L. Tao, Y. Chen and Y. Wei, *RSC Adv.*, 2013, **3**, 21817-21823.
37. X. Zhang, M. Liu, Y. Zhang, B. Yang, Y. Ji, L. Feng, L. Tao, S. Li and Y. Wei, *RSC Adv.*, 2012, **2**, 12153-12155.
38. X. Zhang, Q. Huang, M. Liu, J. Tian, G. Zeng, Z. Li, K. Wang, Q. Zhang, Q. Wan and F. Deng, *Appl. Surf. Sci.*, 2015, **343**, 19-27.
39. Y. Xie, Q. Huang, M. Liu, K. Wang, Q. Wan, F. Deng, L. Lu, X. Zhang and Y. Wei, *RSC Adv.*, 2015, 10.1039/C1035RA08908E.
40. Y. Bulut and H. Karaer, *J. Disper. Sci. Technol.*, 2015, **36**, 61-67.
41. J. Fu, Z. Chen, M. Wang, S. Liu, J. Zhang, J. Zhang, R. Han and Q. Xu, *Chem.Eng. J.*, 2015, **259**, 53-61.
42. J. Z. Sun, A. Qin and B. Z. Tang, *Polym. Chem.*, 2013, **4**, 211-223.
43. B. Yang, Y. Zhao, X. Ren, X. Zhang, C. Fu, Y. Zhang, Y. Wei and L. Tao, *Polym. Chem.*, 2015, **6**, 509-513.
44. T. Madrakian, A. Afkhami, M. Ahmadi and H. Bagheri, *J. Hazard. Mater.*, 2011, **196**, 109-114.
45. X. Ren, B. Yang, Y. Zhao, X. Zhang, X. Wang, Y. Wei and L. Tao, *Polymer*, 2015, **64**, 210-215.
46. Y. Cao, X. Zhang, L. Tao, K. Li, Z. Xue, L. Feng and Y. Wei, *ACS Appl. Mater. Inter.*, 2013, **5**, 4438-4442.
47. Q. Wan, M. Liu, J. Tian, F. Deng, G. Zeng, Z. Li, K. Wang, Q. Zhang, X. Zhang and Y. Wei, *Polym. Chem.*, 2015, **6**, 1786-1792.
48. Q. Wei, F. Zhang, J. Li, B. Li and C. Zhao, *Polym. Chem.*, 2010, **1**, 1430-1433.
49. Y. Shi, M. Liu, K. Wang, F. Deng, Q. Wan, Q. Huang, L. Fu, X. Zhang and Y. Wei, *Polym. Chem.*, 2015, **6**, 5876-5883.
50. Q. Wan, M. Liu, J. Tian, F. Deng, G. Zeng, Z. Li, K. Wang, Q. Zhang, X. Zhang and Y. Wei, *Polym. Chem.*, 2015, **6**, 1786-1792.
51. X. Zhang, G. Zeng, J. Tian, Q. Wan, Q. Huang, K. Wang, Q. Zhang, M. Liu, F. Deng and Y. Wei, *Appl. Surf. Sci.*, 2015, **351**, 425-432.

52. L. Xu, N. Liu, Y. Cao, F. Lu, Y. Chen, X. Zhang, L. Feng and Y. Wei, *ACS Appl. Mater. Inter.*, 2014, **6**, 13324-13329.
53. J. Cui, Y. Yan, G. K. Such, K. Liang, C. J. Ochs, A. Postma and F. Caruso, *Biomacromolecules*, 2012, **13**, 2225-2228.
54. M. Liu, J. Ji, X. Zhang, X. Zhang, B. Yang, F. Deng, Z. Li, K. Wang, Y. Yang and y. wei, *J. Mater. Chem. B*, 2015, **3**, 3476 - 3482.
55. X. Zhang, S. Wang, L. Xu, L. Feng, Y. Ji, L. Tao, S. Li and Y. Wei, *Nanoscale*, 2012, **4**, 5581-5584.
56. J. Tian, D. Xu, M. Liu, F. Deng, Q. Wan, Z. Li, K. Wang, X. He, X. Zhang and Y. Wei, *J. Polym. Sci. Polym. Chem.*, 2015, **53**, 1872-1879.
57. S. M. Kang, S. Park, D. Kim, S. Y. Park, R. S. Ruoff and H. Lee, *Adv. Funct. Mater.*, 2011, **21**, 108-112.
58. H. C. Yang, J. Luo, Y. Lv, P. Shen and Z. K. Xu, *J. Membrane Sci.*, 2015, **483**, 42-59.
59. X. Zhang, K. Wang, M. Liu, X. Zhang, L. Tao, Y. Chen and Y. Wei, *Nanoscale*, 2015, **7**, 11486-11508.
60. C. Cheng, S. Li, J. Zhao, X. Li, Z. Liu, L. Ma, X. Zhang, S. Sun and C. Zhao, *Chem.Eng. J.*, 2013, **228**, 468-481.
61. Z. Dong, D. Wang, X. Liu, X. Pei, L. Chen and J. Jin, *J. Mater. Chem. A*, 2014, **2**, 5034-5040.
62. Q. Wan, J. Tian, M. Liu, G. Zeng, Q. Huang, K. Wang, Q. Zhang, F. Deng, X. Zhang and Y. Wei, *Appl. Surf. Sci.*, 2015, **346**, 335-341.
63. Q. Wan, M. Liu, J. Tian, F. Deng, Y. Dai, K. Wang, Z. Li, Q. Zhang, X. Zhang and Y. Wei, *RSC Adv.*, 2015, **5**, 38316-38323.
64. J. Fu, Z. Chen, M. Wang, S. Liu, J. Zhang, J. Zhang, R. Han and Q. Xu, *Chem. Eng. J.* , 2015, **259**, 53-61.
65. J. Chang, J. Ma, Q. Ma, D. Zhang, N. Qiao, M. Hu and H. Ma, 2015, 10.1016/j.clay.2015.1006.1038.